ChemComm

COMMUNICATION

View Article Online
View Journal | View Issue



Cite this: *Chem. Commun.*, 2015, **51**, 7512

Received 22nd February 2015,
Accepted 23rd March 2015

DOI: 10.1039/c5cc01592h

www.rsc.org/chemcomm

# Twist grain boundary (TGB) states of chiral liquid crystalline bent-core mesogens†

Hale Ocak,*[ab] Belkız Bilgin-Eran,[b] Dilek Güzeller,[b] Marko Prehm[a] and Carsten Tschierske*[a]

**4-Cyanoresorcinol derived bent-core molecules with a chiral (*S*)-2-methylbutoxy chain form liquid crystalline phases with TGBA- and TGBC-like structures at the transition from cybotactic nematic *via* SmA to SmC phases.**

Chirality has huge effects on molecular self-assembly.[1] Soft matter, especially liquid crystalline (LC) phases,[2,3] can easily be affected by chirality leading to helical superstructures.[4] Molecules with high helical twisting power‡ can even give rise to the frustration of the fundamental structures of LC self-assembly, thus providing new superstructures with a higher level of complexity[3] and new emerging properties. Examples are the three-dimensional lattices of defects in the blue phases which are of importance as photonic band gap materials and represent candidates for new generations of extremely fast switching electro-optical devices,[5] twist grain boundary (TGB) phases,[6] representing analogues of the Abrikosov flux phase of type-II superconductors[7] and several other complex structures.[5,8]

TGB phases, formed by chiral rod-like mesogens, represent helical superstructures with a helix axis parallel to the layer planes thus disrupting the layers to give blocks separated by screw dislocations (Fig. 1). TGB phases can be divided into TGBA phases with an orthogonal organization of the molecules with respect to the planes of these blocks and several different modes of TGBC phases with a tilted organization of the molecules.[6] In the recent two decades bent-core (BC) molecules[9] have attracted special attention as new LC materials. This is mainly due to their capability to form LC phases with polar order[9] and the spontaneous formation of chiral superstructures though the molecules are achiral.[9–12] An interesting point concerns the interaction of these chiral superstructures with the molecular chirality provided by stereogenic units. For example, enhancement of chirality was observed by doping chiral LC phases with achiral bent-core mesogens, which lead to the induction of highly frustrated blue phases with helical organization in all three directions instead of only one in the cholesteric phases.[5] It was proposed that "highly chiral" conformations[11,13] of the bent aromatic cores lead to a high twisting power.‡ For the same reason broad regions of blue phases were recently found for optically active BCLCs.[14]

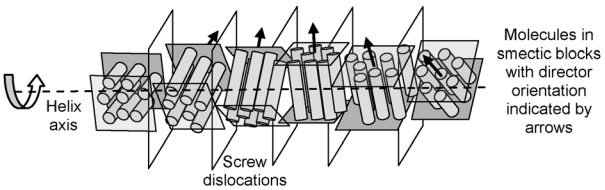


Fig. 1 Schematic image of the twist grain boundary (TGB) structure.

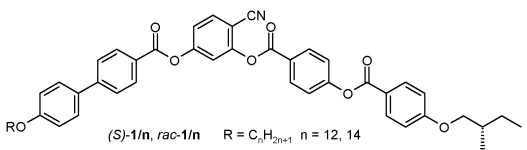


Herein we report the first observation of TGB-like structures for the LC phases of the BC mesogens (*S*)-**1/*n*** ($n$ = 12, 14) involving a 4-cyanoresorcinol derived BC,[14b,15] combined with a chiral (*S*)-2-methylbutoxy group. In order to identify the specific chirality effects, one of the compounds was also synthesized in racemic form (*rac*-**1/12**). The synthetic strategy of these BC compounds is outlined in Scheme 1 and the experimental procedures are described in the ESI.†

The observed LC phases, their transition temperatures and associated enthalpies are collated in Table 1. Upon cooling the racemic mixture *rac*-**1/12** from the isotropic liquid (Iso) a nematic phase (N) is formed at first which is then replaced by a lamellar phase (SmA) at $T \leq 96$ °C. In the SmA phase there is on average a non-tilted organization of the molecules in layers, whereas at the transition to the SmC phase at $T = 88$ °C a uniform tilt develops. In calorimetric investigations besides the dominating melting peak

[a] *Institute of Chemistry, Organic Chemistry, Martin-Luther University Halle-Wittenberg, Kurt-Mothes Str. 2, 06120 Halle, Germany. E-mail: carsten.tschierske@chemie.uni-halle.de; Fax: +49 345 5527346*
[b] *Department of Chemistry, Yildiz Technical University, Davutpasa Yerlesim Birimi, TR-34220, Esenler, Istanbul, Turkey. E-mail: ocak_hale@hotmail.com; Fax: +90 212 3834134*

† Electronic supplementary information (ESI) available: Synthesis of compounds, analytical data, DSC traces, additional XRD patterns, textures and other data. See DOI: 10.1039/c5cc01592h

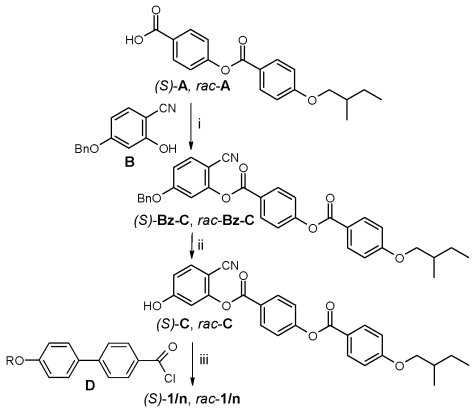


Scheme 1 Synthesis of **1/*n***. *Reagents and conditions*: (i) DCC, DMAP, $CH_2Cl_2$, 20 °C; (ii) $H_2$, Pd/C, THF, 40 °C; (iii) pyridine, $CH_2Cl_2$, 20 °C, ESI.†

Table 1 Transitions of the investigated compounds[a]

| Comp. | $T$/°C [$\Delta H$/kJ mol$^{-1}$] |
|---|---|
| *rac*-**1/12** | Cr 95 [34.7] (SmC 88 [<0.01]) SmA 96 [<0.01] $N_{cybA}$ 108 [1.1] Iso |
| (*S*)-**1/12** | Cr 98 [39.3] (SmC*/TGBC 88 [<0.01] TGBA 96 [<0.01]) $N^*_{cybA}$ 108 [1.2] Iso |
| (*S*)-**1/14** | Cr 99 [44.9] (SmC*/TGBC 94 [<0.01]) TGBA 102 [<0.01] $N^*_{cybA}$ 109 [1.4] Iso |

[a] Transition temperatures and enthalpy values (square brackets) determined by DSC (1st heating and cooling, rates 10 K min$^{-1}$, peak temperatures) or by PM for transitions without visible $\Delta H$; round brackets indicate monotropic (metastable) phases; abbreviations: Cr = crystalline solid; Iso = isotropic liquid; $N_{cybA}$ = cybotactic nematic phase composed of SmA clusters; $N^*_{cybA}$, SmC* = chiral $N_{cybA}$ and SmC phases, respectively; SmA = non-tilted smectic phase; SmC = synclinic tilted smectic phase; TGB = twisted states of the SmA (TGBA) or SmC phases (TGBC) with the helix axis parallel to the layers; for DSCs see Fig. S7 (ESI).

only the Iso–N transition could be observed by a small DSC peak (~1.1 kJ mol$^{-1}$), whereas there is no measurable enthalpy change for the other LC phase transitions (Fig. S7, ESI†). This indicates that major structural transformations take place at the Iso–N transition and this is in line with a cybotactic structure of the nematic phase, as confirmed by XRD ($N_{cybA}$, see below).[15b] It appears that the following phase transitions are continuous and mainly associated with the growth of the cybotactic clusters. All samples can be cooled to about 60 °C without crystallization, so that the monotropic LC phases can also be easily investigated (see Table 1).

The phase transition temperatures of the (*S*)-enantiomer (*S*)-**1/12** are the same as those found for *rac*-**1/12**. For (*S*)-**1/14** a very similar behaviour to those for (*S*)-**1/12** is observed, only the transitions between the LC phases occur at a bit higher temperatures (Table 1). The typical textures observed for the LC phases of (*S*)-**1/*n*** (*n* = 12, 14) are shown in Fig. 2. A cholesteric oily-streak texture indicates the presence of a helical superstructure in the chiral nematic phases (N*) (Fig. 2a).[5] The appearance of the LC phases occurring below N* strongly depends on the alignment conditions. Homeotropic anchoring (layers parallel to the surfaces of the glass substrates) leads to filament textures, as characteristic for TGBA phases[16] (Fig. 2b). The filaments rapidly disappear and the textures become uniformly dark, indicating the transition to an optically uniaxial SmA phase. Upon further cooling, a gray and low birefringent texture develops in these homeotropic samples, indicating a transition to a SmC* phase, occurring for (*S*)-**1/12** at about the same temperature as observed for the SmA–SmC transition of the racemate.§ In a cell with planar surface anchoring (layers perpendicular to the substrate surfaces; polyimide-coated ITO cell, 10 μm) the cholesteric oily streak texture changes at the N*–SmA transition to a planar texture composed of differently coloured areas,

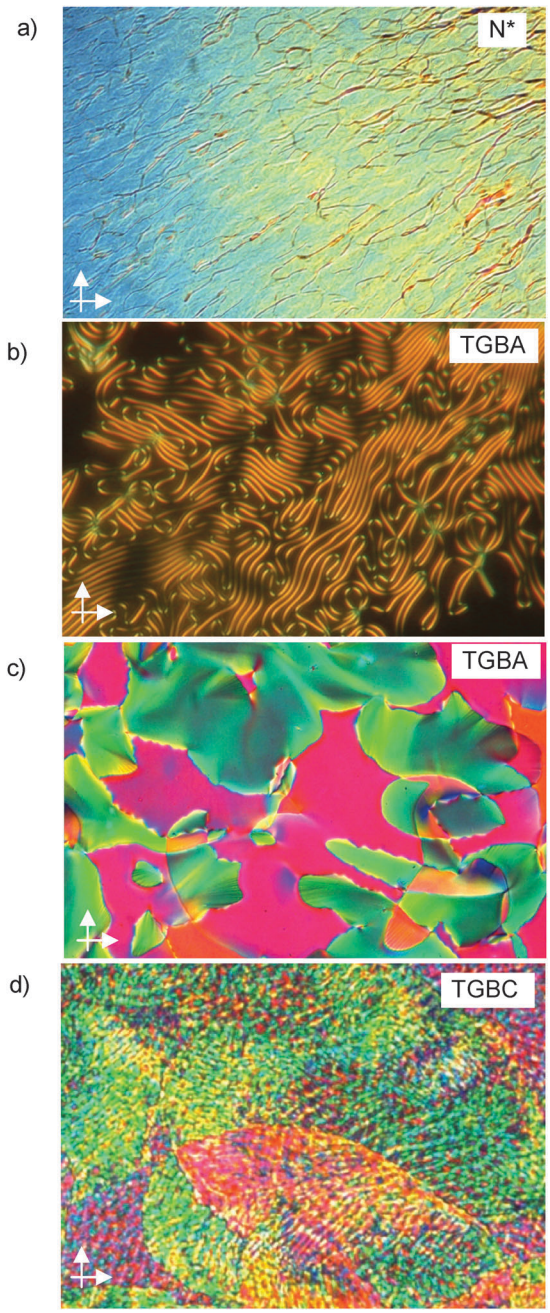


Fig. 2 Textures of the LC phases of compounds (*S*)-**1/*n*** between crossed polarisers: (a) oily-streak texture of the N* phase of (*S*)-**1/14** at $T$ = 107 °C; (b) fingerprint texture of (*S*)-**1/14** in the TGBA-state in homeotropic anchoring at $T$ = 96 °C, (c) TGBA-state of (*S*)-**1/12** in planar anchoring (polyimide coated ITO-cell, 10 μm) at $T$ = 92 °C and (d) TGBC-like texture at $T$ = 79 °C; for additional textures see Fig. S2–S5 (ESI†).

corresponding to different twist states (Fig. 2c). This texture, which is typical for TGBA phases, is retained upon further cooling (see Fig. S2, ESI†) and at the SmA/SmC phase transition temperature the formation of a grid-like pattern is observed (Fig. 2d), similar to textures of TGBC phases.[4,6,17] The texture continuously changes upon further cooling (see Fig. S3, ESI†). Therefore it is not clear if the TGBC structure is retained or a slow transition to a SmC*-phase takes place upon further cooling (therefore it is denoted as SmC*/TGBC in Table 1).

XRD investigations were performed for (*S*)-**1/12** and *rac*-**1/12** in thin capillaries at a magnetic field $B \sim 1$ T after slow cooling (0.1 K min$^{-1}$) from the isotropic liquid. In the whole investigated temperature range between 60 and 110 °C the wide angle scattering is diffuse indicating the presence of LC phases without long range order between individual molecules (Fig. 3a and b). In the small angle range there is a diffuse scattering in the N and N* phases, exceeding the wide angle scattering and thus confirming cybotactic nematic phases composed of smectic clusters.[15b] For *rac*-**1/12** the small angle scattering maximum is on the meridian, indicating that the molecules have no uniform tilt in these domains, *i.e.* the nematic phases are composed of SmA clusters ($N_{cybA}$), which is rarely found for BC molecules.[15b] The intensity of the small angle scattering increases further at the transition to the SmA phase (Fig. 3d). The *d*-spacings of 4.05–4.10 nm, corresponding to ~0.85 molecular length ($L_{mol}$ = 4.8 nm in the most stretched conformation, see Fig. S8, ESI†), are in line with a single layer structure of the cybotactic clusters and layers. The $d = f(T)$ plot for *rac*-**1/12** indicates an increase of *d* in the N and SmA phases due to an increasing packing density, leading to alkyl chain stretching. A slight decrease of *d* starts at around the SmA–SmC transition, in line with the onset of uniform tilt at this transition (Fig. 3c). The tilt in the SmC phase is very small (<5°) as estimated for *rac*-**1/12** from the angle between the diffuse wide angle scattering maxima on the equator and the layer reflections on the meridian (XRD tilt). The optical tilt is about 10–15° as estimated from the planar textures of *rac*-**12** (see Fig. S1g and h, ESI†), indicating that the main contribution comes from the tilt of the aromatic cores.

The LC phases of (*S*)-**1/12** (Fig. 3b) have approximately the same *d*-values as those of *rac*-**1/12**. However, in the N* phase the small- and wide-angle scatterings form closed rings, indicating the absence of uniform alignment due to the presence of the helical superstructure. At the transition to TGBA the rings condense to crescent like maxima on the meridian (small angle) and on the equator (wide angle), respectively, in line with the formation of layers. There is a broader angular $\chi$-distribution of the scattering in the smectic phases of (*S*)-**1/12** compared to the sharper peak of *rac*-**1/12** (Fig. 3a and b). However, there is no distribution of the scatterings on a closed ring as it would be expected for TGB phases. So, there seems to be a strong effect of the conditions on the actually observed phase structure. As shown above, planar anchoring stabilizes the TGB helix, whereas homeotropic anchoring has the opposite effect; it stabilizes the layers and tends to remove the TGB helix. Hence, the TGB structures are not considered as "phases", but as helically deformed states of the underlying smectic phases. The reduced influence of surface anchoring in the capillaries used for XRD, and the alignment of the molecules by the magnetic field, might

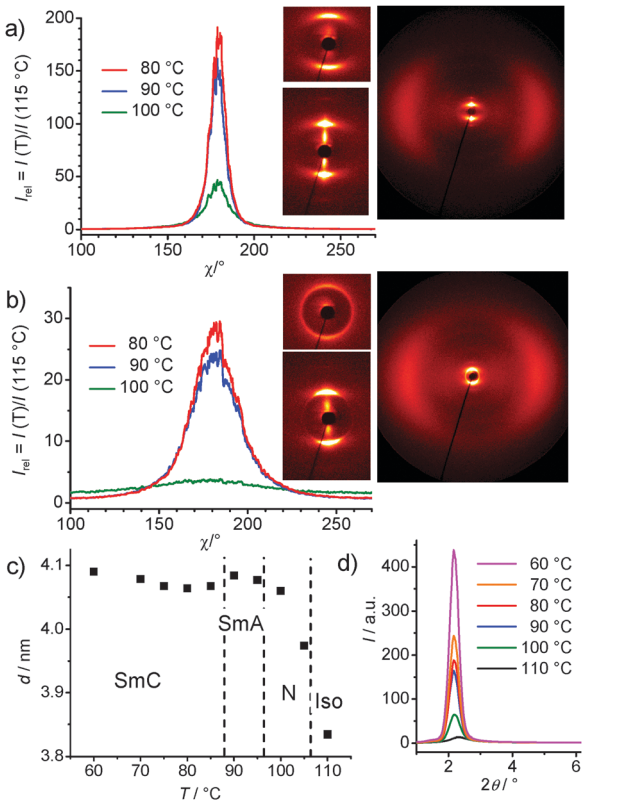


Fig. 3 XRD data (a, c, d) of *rac*-**1/12** and (b) of (*S*)-**1/12**. (a, b) $\chi$-scans over the small angle scattering depending on *T* and corresponding 2D XRD patterns of magnetically aligned samples in the N/N* phase at *T* = 105 °C (top left) and in the tilted smectic phases (bottom and right) at *T* = 80 °C; (c) *T*-dependence of the *d*-spacing and (d) 2$\theta$-scan over the small angle scattering depending on *T*, see Tables S1, S2 and Fig. S9, S10 (ESI†).

suppress TGB-helix formation. The broader angular distribution of the scattering of (*S*)-**1/12** might be due to the remaining helical layer distortion or to the less efficient alignment obtained by cooling from the N* phase.

There is no polarization current response under a triangular wave field (PI coated ITO cells 10 μm) in the temperature range of all mesophases for the racemic mixtures as well as for the (*S*)-enantiomers up to the maximum available value of ±28 V μm$^{-1}$, indicating the absence of polar order.¶

As an additional interesting point, it should be noted that chiral domains are visible in homeotropic alignment in the range of the SmC phase of the racemic compound *rac*-**1/12**. These domains can be identified by slight rotation of the analyzer either clockwise or anti-clockwise out of the precise 90° orientation, which reverses the brightness of these domains (Fig. 4a–c).[9,11,13] Rotating the sample between the polarizers does not lead to such a change in brightness, thus excluding tilt director alignment as the origin of this effect (Fig. S6, ESI†). In addition, though domains can also be recognized in the homeotropic SmC* phase of (*S*)-**1/12**, in this case there is no visible effect of the orientation of the polarizer (Fig. 4d–f). As there is no polar order in the SmC phase the origin of chirality must be due to the segregation of chiral molecular conformers,[13] which is additionally supported by surface interaction.‖ This indicates a strong chirality of the molecular conformations and a strong

 

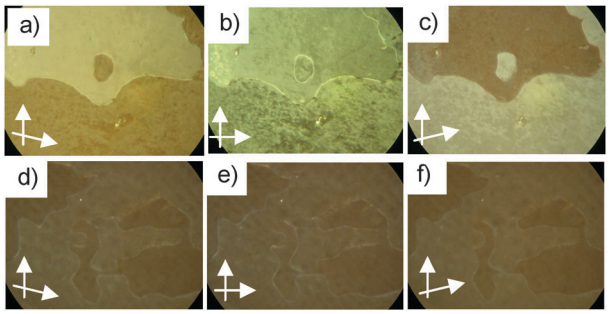


Fig. 4 Textures of the homeotropic SmC phases (a–c) of *rac*-**1/12** and (d–f) of (*S*)-**1/12** at $T$ = 75 °C as observed (b,e) between crossed polarizers and between uncrossed polarizers with the analyzer rotated by 5° (a, d) clockwise or (c, f) counter-clockwise; reversal of brightness in the series (a–c) indicates chiral domains with opposite handedness, whereas there is no effect in the series (d–f) (see also Fig. S6, ESI†).

coupling between them. The cybotactic nature of the nematic phase and the absence of clear transition enthalpies at the phase transitions indicate a nearly continuous growth of the coherence length of the smectic clusters throughout the $N_{cybA}$–SmA–SmC transitions (Fig. 3d, Table S1, ESI†). This indicates that already in the nematic phase the cybotactic clusters are relatively large and continue to increase in the smectic phases. Thus, in the SmA and SmC phases there is a remaining layer distortion providing soft layers which can be easily deformed into a TGB-like superstructure (Fig. 1). Therefore, the weak helical twisting power of the (*S*)-2-methylbutyl group can provide a sufficiently strong chirality effect such that TGB states are formed at the N*–SmA transition. These can be further stabilized over broader temperature ranges by planar surface anchoring.

In summary, the first observation of TGB structures in mesophases of bent-core mesogens is reported.** These are formed by molecules with a (*S*)-2-methylbutoxy stereogenic centre, known to have only weak helical twisting power. However, strong chirality of the molecular conformers, an imperfect layer structure and surface anchoring can stabilize the TGB states.

The work was supported by DFG (Ts 39/24-1); H. O. is grateful to the Alexander von Humboldt Foundation for a research fellowship at Martin Luther University, Halle-Wittenberg; B. B.-E. is grateful to the Alexander von Humboldt Foundation for financial support toward LC research.

## Notes and references

‡ The helical twisting power is an empirical measure of the effect of chirality on LC superstructures. It depends on molecular structural parameters, conditions (*e.g.* $T$), enantiomeric purity and the type of superstructure. It is inversely proportional to the helical pitch and depends on the helicity of the molecular conformations, the energy barriers between enantiomorphic conformers and the degree of coupling of the stereogenic unit with the molecular conformational helicity.[5]

§ The birefringence in the homeotropic SmC* phases is much lower than in the SmC phase of *rac*-**12** (see Fig. 4), indicating the presence of a helix along the layer normal being larger than the wavelength of light.

¶ That no switching peak could be observed even in the SmC* phases could be due to the known weak effect of the (*S*)-2-methylbutyl group on polar order, leading to very small values of spontaneous polarization.[5,14b] Also optically, no switching can be observed; this confirms that there is no switching or it takes place by rotating around the molecular long axis.

‖ This kind of chiral SmC phase was previously reported for 4-cyanoresorcinol based BC molecules with azobenzene wings, and a local $SmC_sP_F$ structure was assumed to be responsible for chirality.[18] However the recent observation of chiral segregation in isotropic liquids[13] supports the possibility of spontaneous chiral segregation in SmC phases with a dense packing of the aromatic cores. This chiral segregation provides a helical distortion of the layers, thus giving rise to layer distortion and leading to amplification of small chirality effects.

** TGB-like twist states and TGB phases were observed for mixtures of chiral rod-like molecules with achiral bent-core molecules[19] or hockey-stick compounds[20] and for chiral dimesogens with odd spacers.[17] A TGB-like structure has also been discussed as a possible organization in the dark conglomerate (DC) phases of achiral BC molecules,[21a] but only recently a DC-like random grain boundary phase of achiral hockey-stick LC was reported.[21b]

1 D. B. Amabilino, *Chirality at the Nanoscale*, Wiley-VCH, Weinheim, 2009.
2 *Handbook of Liquid Crystals*, ed. J. W. Goodby, P. J. Collings, T. Kato, C. Tschierske, H. F. Gleeson and P. Raynes, Wiley-VCH, Weinheim, 2014.
3 C. Tschierske, *Angew. Chem., Int. Ed.*, 2013, **52**, 8828–8878.
4 I. Dierking, *Symmetry*, 2014, **6**, 444–472.
5 *Chirality in liquid crystals*, ed. H.-S. Kietzerow and C. Bahr, Springer, New York. NY, 2001.
6 (*a*) J. W. Goodby, M. A. Waugh, S. M. Stein, E. Chin, R. Pindak and J. S. Patel, *Nature*, 1989, **337**, 449–452; (*b*) J. W. Goodby, *Curr. Opin. Colloid Interface Sci.*, 2002, **7**, 326–332; (*c*) M. Brunet, L. Navailles and N. A. Clark, *Eur. Phys. J. E: Soft Matter Biol. Phys.*, 2002, **7**, 5–11.
7 S. R. Renn and T. C. Lubensky, *Phys. Rev. A: At., Mol., Opt. Phys.*, 1988, **38**, 2132–2147.
8 H. T. Nguyen, M. Ismaili, N. Isaert and M. F. Achard, *J. Mater. Chem.*, 2004, **14**, 1560–1566.
9 (*a*) R. A. Reddy and C. Tschierske, *J. Mater. Chem.*, 2006, **16**, 907–961; (*b*) H. Takezoe and Y. Takanishi, *Jpn. J. Appl. Phys.*, 2006, **45**, 597–625; (*c*) A. Eremin and A. Jakli, *Soft Matter*, 2013, **9**, 615.
10 L. E. Hough, M. Spannuth, M. Nakata, D. A. Coleman, C. D. Jones, G. Dantlgraber, C. Tschierske, J. Watanabe, E. Körblova, D. M. Walba, J. E. Maclennan, M. A. Glaser and N. A. Clark, *Science*, 2009, **325**, 452.
11 H. Takezoe, *Top. Curr. Chem.*, 2012, **318**, 303–330.
12 V. P. Panov, R. Balachandran, J. K. Vij, M. G. Tamba, A. Kohlmeier and G. H. Mehl, *Appl. Phys. Lett.*, 2012, **101**, 234106.
13 C. Dressel, T. Reppe, M. Prehm, M. Brautzsch and C. Tschierske, *Nat. Chem.*, 2014, **6**, 971–977.
14 (*a*) H.-C. Jeong, S. Aya, S. Kang, F. Araoka, K. Ishikawa and H. Takezoe, *Liq. Cryst.*, 2013, **40**, 951–958; (*b*) H. Ocak, B. Bilgin-Eran, M. Prehm, S. Schymura, J. P. F. Lagerwall and C. Tschierske, *Soft Matter*, 2011, **7**, 8266–8280.
15 (*a*) L. Kovalenko, M. W. Schröder, R. A. Reddy, S. Diele, G. Pelzl and W. Weissflog, *Liq. Cryst.*, 2005, **32**, 857–865; (*b*) C. Keith, A. Lehmann, U. Baumeister, M. Prehm and C. Tschierske, *Soft Matter*, 2010, **6**, 1704–1721.
16 I. Dierking and S. T. Lagerwall, *Liq. Cryst.*, 1999, **26**, 83–95.
17 C. V. Yelamaggad, A. S. Achalkumar, N. L. Bonde and A. K. Prajapati, *Chem. Mater.*, 2006, **18**, 1076–1078.
18 M. Alaasar, M. Prehm, M. Nagaraj, J. K. Vij and C. Tschierske, *Adv. Mater.*, 2013, **25**, 2186–2191.
19 P. Archer and I. Dierking, *Liq. Cryst.*, 2006, **33**, 257–265.
20 V. Novotna, M. Glogarova, V. Kozmik, J. Svoboda, V. Hamplova, M. Kaspar and D. Pociecha, *Soft Matter*, 2013, **9**, 647–653.
21 (*a*) S. K. Lee, L. Shi, M. Tokita and J. Watanabe, *J. Phys. Chem. B*, 2008, **112**, 6762–6766; (*b*) D. Chen, H. Wang, M. Li, M. A. Glaser, J. E. Maclennana and N. A. Clark, *Soft Matter*, 2014, **10**, 9105–9109.